PROCEEDINGS OF SCIENCE

New Constraint for Isotropic Lorentz Violation from LHC Photon Data

David Amram[a,*]

[a] *IP2I Lyon,*
4 rue Enrico Fermi, Villeurbanne, France

E-mail: david.amram@cern.ch

We present new calculations for the kinematics of photon decay into fermion pairs in vacuum, considering an isotropic Lorentz invariance violation (LV) as described by the Standard-Model Extension (SME). These calculations are applied to the interpretation of prompt photon production in LHC data. The inclusive measurement of prompt photon production at the LHC Run 2, with photon transverse energies reaching 2.5 TeV, leads to a lower bound on the isotropic coefficient, $\tilde{\kappa}_{tr} > -1.06 \times 10^{-13}$ at 95% confidence level. This improves the previous collider constraint by a factor of 55. Additionally, the derived kinematics of photon decay can be utilized to further constrain LV coefficients through the detection of fermion pair production, such as top-antitop events.

9th Symposium on Prospects in the Physics of Discrete Symmetries (DISCRETE2024)
2–6 Dec 2024
Ljubljana, Slovenia

*Speaker

 ISSN 1824-8039 . Published by SISSA Medialab.

PoS(DISCRETE2024)001

1. Introduction

Lorentz invariance is a fundamental symmetry in both the Standard Model (SM) of particle physics and General Relativity (GR). The search for Lorentz invariance violation (LV) is driven by the ongoing efforts to reconcile Quantum Field Theory (QFT) with Quantum Gravity (QG). Direct experimental probes of QG at Planck scales energies remain impractical. An alternative approach is to investigate tiny deviations from Lorentz symmetry at relatively lower, yet accessible, energies, for instance in high-energy physics experiments.

The Standard-Model Extension (SME) [1, 2] offers a model-independent framework to describe small LV effects, which are predicted in various theories, including string field theory, loop quantum gravity, non-commutative field theory, spacetime foam models, and Horava-Lifshitz gravity. The SME is an effective field theory that includes all particles of the Standard Model, preserves the gauge symmetries of the Standard Model, and incorporates every possible term that breaks Lorentz invariance. It provides a parametrization of deviations from Lorentz invariance through coefficients that quantify the magnitude of these effects.

The SME introduces 19 independent coefficients in the Lagrangian for electromagnetism that remain constant under Lorentz transformations, thereby breaking Lorentz invariance. This leads to a modified dispersion relation and effects such as photon decay in vacuum and Cherenkov radiation, providing observable signatures for experimental searches. Isotropic Lorentz violation is characterized by a single degree of freedom, describing spatially isotropic LV effects. While isotropic effects of LV are mainly constrained by astrophysics [3], high-energy earth-based laboratory experiments are less model dependent and use a controlled source of particles, allowing more conservative limits on LV effects. These proceedings are highlighting the results obtained in Ref. [4].

2. Kinematic

We consider a modified quantum electrodynamics (QED) framework that incorporates Lorentz violation (LV) in the photon sector. The Lagrangian of the theory is modified by introducing a rank-4 Lorentz-violating tensor $\kappa^{\mu\nu\rho\sigma}$:

$$\mathcal{L}_{\text{SME}} = -\frac{1}{4}(\eta^{\mu\varrho}\eta^{\nu\sigma} + \kappa^{\mu\nu\varrho\sigma})F_{\mu\nu}(x)F_{\varrho\sigma}(x) + \frac{1}{2}\bar{\psi}(x)(\gamma^{\mu}iD_{\mu} - m_f)\psi(x) \tag{1}$$

The physics of Eq.1 is characterized by a nontrivial refractive index of the vacuum, resulting in a speed of light that differs from the maximum velocity of Dirac particles. While the refractive index could exhibit anisotropy or polarization dependence, such effects are tightly constrained by spectropolarimetry measurements [3], leading to the exclusion of birefringent components. The remaining non-birefringent Lorentz violation is parametrized by a symmetric, traceless matrix $\tilde{\kappa}_{\mu\nu}$, with isotropic Lorentz violation in the laboratory frame described by a single coefficient [5], $\tilde{\kappa}_{\text{tr}}$:

$$\kappa^{\mu\nu} = \frac{3}{2}\tilde{\kappa}_{\text{tr}}\text{diag}\left(1, \frac{1}{3}, \frac{1}{3}, \frac{1}{3}\right)^{\mu\nu}. \tag{2}$$

This modification leads to a modified dispersion relation for photons:

$$\omega = A|k|, \quad A = \sqrt{\frac{1-\tilde{\kappa}_{\text{tr}}}{1+\tilde{\kappa}_{\text{tr}}}}, \tag{3}$$

where k is the three-momentum of the photon.

Two distinct physical regimes emerge from this framework. For $\tilde{\kappa}_{\rm tr} \in (0,1)$, the group velocity of photons satisfies $v_{\rm gr} < 1$, while the dispersion relation for Dirac fermions remains standard for massive particles. This implies that fermions can potentially propagate faster than light. For $\tilde{\kappa}_{\rm tr} \in (-1,0)$, the group velocity of photons satisfies $v_{\rm gr} > 1$, meaning photons always travel faster than fermions, regardless of their energy. In the first regime ($\tilde{\kappa}_{\rm tr} \in (0,1)$), vacuum Cherenkov radiation can occur, while in the second regime ($\tilde{\kappa}_{\rm tr} \in (-1,0)$), photon decay in vacuum becomes a characteristic process. We will focus on the latter one.

The photon decay in vacuum is governed by a threshold energy, derived as [6]:

$$E_{\rm th} = 2m_f \sqrt{\frac{1-\tilde{\kappa}_{\rm tr}}{-2\tilde{\kappa}_{\rm tr}}}, \tag{4}$$

where m_f is the mass of the fermion. When the photon energy exceeds the threshold, the excess energy allows the final-state particles to be emited at a nonzero θ angle. This angle is determined by [4]:

$$\cos\theta = \frac{E_f(E_\gamma - E_f) + \frac{\tilde{\kappa}\mathrm{tr}}{1-\tilde{\kappa}\mathrm{tr}} E_\gamma^2 + m_f^2}{\sqrt{(E_f^2 - m_f^2)[(E_\gamma - E_f)^2 - m_f^2]}}, \tag{5}$$

where E_γ and E_f represent the energies of the incoming photon and outgoing fermion, respectively. The antifermion's energy is fixed by energy-momentum conservation.

In the example of a photon decaying to a top quark-antiquark pair, we obtain a kinematic different from that of the SM $pp \to t\bar{t}$ processes, illustrated in Fig 1 via the opening angle between top quarks for several threshold energies. A new result is the partial decay width with respect to the fermion's energy can be expressed as [4]:

$$\frac{d\Gamma}{dE_f} = \frac{\alpha}{(1+\tilde{\kappa}\mathrm{tr})^2\sqrt{1-\tilde{\kappa}\mathrm{tr}^2}} \frac{1}{E_\gamma^2} \left[(1-\tilde{\kappa}\mathrm{tr})[2\tilde{\kappa}\mathrm{tr} E_f(E_\gamma - E_f) + (1+\tilde{\kappa}\mathrm{tr})m_f^2] - \tilde{\kappa}\mathrm{tr} E_\gamma^2 \right]. \tag{6}$$

3. Experimental search for photon decaying in vacuum

The ATLAS experiment at the LHC measured high-energy prompt photon data, ideal for testing Lorentz violation. We reinterpret the ATLAS inclusive measurement of prompt photon at a center-of-mass energy of 13 TeV [7], with photons observed up to a transverse energy of 2.5 TeV. In the context of LV, photons above a certain energy threshold are expected to decay. If photons decay within the detector range, a deficit in high-energy photon counts would be expected.

A Monte Carlo (MC) simulation of prompt photon production in the process $p\,p \to \gamma$ + jet was performed at tree level, incorporating up to 3 additional partons at leading order in perturbative QCD. The SHERPA generator v.2.2.15 [8, 9] was used, and the resulting events were reweighted to match the ATLAS MC distribution. We select events where the transverse energy of the photon satisfies $E_T^\gamma > 125$ GeV and its pseudorapidity remains within $|\eta^\gamma| < 0.6$. The photon isolation criteria are determined using the RIVET routine, following the approach of a previous 8 TeV analysis

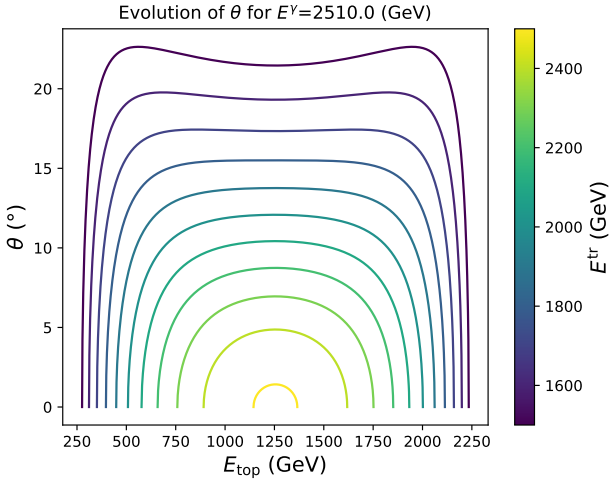

Figure 1: Illustration of the opening angle of top-antitop pairs from the decay of a photon of 2510 GeV in the presence of Lorentz violation at different threshold energies.

[10]. These same criteria are applied in the 13 TeV study [7]. Among the photons in each selected event, the one with the highest transverse energy is retained. Assuming photons decay to electrons, we can compute the probability of a photon to decay as $1 - e^{-\Gamma x}$, where Γ is the total decay width obtained by integrating Eq. 6 over the allowed domain of energy defined in Ref. [4], and x is the distance to the detector.

However, a decayed photon could still impact the measured E_T distribution if an electron produced from the photon decay is misidentified as a photon. In the ATLAS measurement, the photon identification uncertainty is less than 1.5% [7]. We assign this value to the probability of an electron to be reconstructed as a photon. A single electron passing this probability will have its E_T drawn accordingly to Eq. 6 and included in the E_T^γ distribution. If both electrons are reconstructed as a photon, only the largest transverse energy is included.

The constraint on $\tilde{\kappa}_{tr}$ was derived using the CLs method [11], comparing the likelihood of the SM-only hypothesis against the SM+LV hypothesis, assuming a Poisson distribution for the number of events in each bin. The number of observed events is computed such as:

$$N_i = \frac{d\sigma_i}{dE_T^\gamma} \cdot \Delta E_{T,i}^\gamma \cdot \epsilon \cdot L \tag{7}$$

where $\Delta E_{T,i}^\gamma$ is the bin width, ϵ the photon reconstruction and identification efficiency and L the integrated luminosity. The analysis incorporates systematic uncertainties from ATLAS data, including sources from background subtraction, unfolding, pile-up trigger efficiency, luminosity measurement and photon energy scale and resolution. Each of those uncertainties is added in quadrature and treated conservatively as a separate Gaussian nuisance parameter for each bin. To set the limit on $\tilde{\kappa}_{tr}$, we performed a serie of simulations under a range of assumptions for the LV parameter $\tilde{\kappa}_{tr}$. The impact on the E_T^γ distribution of the variation of the $\tilde{\kappa}_{tr}$ parameter is shown in Fig 2. This allows us to construct a CL_s curve as a function of $\tilde{\kappa}_{tr}$. Fig 3 illustrates these results, with a linear interpolation applied between computed points to provide a continuous constraint on

$\tilde{\kappa}_{tr}$. Using the conventional criterion of $CL_s < 0.05$, the resulting 95% confidence level bound is:

$$\tilde{\kappa}_{tr} > -1.06 \times 10^{-13} \tag{8}$$

This corresponds to a threshold energy of $E^{th} = 2.2218$ TeV. The previous limit from collider physics was set by reinterpreting D0 data [12] as $\tilde{\kappa}_{tr} > -5.8 \times 10^{-12}$ [13]. This new bound represents an improvement of a factor 55 over the previous one.

4. Conclusions and Perspectives

These proceedings are presenting results obtained in Ref. [4]. We have presented a new calculation of the kinematics of photon decay into fermions in vacuum under an isotropic violation of Lorentz invariance. This theoretical framework, based on the Standard-Model Extension (SME), predicts a modified dispersion relation for photons, allowing for their decay into massive fermion pairs if Lorentz symmetry is violated. By applying this formalism to high-energy photon data from the LHC, we have set a new constraint on the isotropic SME coefficient $\tilde{\kappa}_{tr} > -1.06 \times 10^{-13}$ at 95% confidence level. This result represents a significant improvement by a factor of 55 over the previous collider-based bound established using D0 data.

The case of photon decay to top quark pairs illustrates the impact of Lorentz violation on kinematics, showing distinct deviations from Standard Model predictions. Our results not only reinforce the potential of collider experiments in probing fundamental symmetries but also demonstrate the viability of reinterpretations of LHC data to set stringent limits on new physics beyond the Standard Model. Unlike astrophysical constraints, which often rely on model-dependent assump-

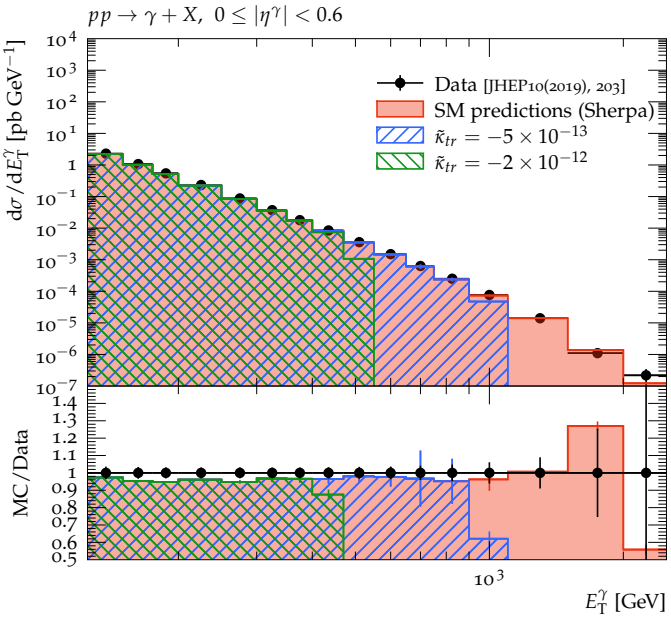

Figure 2: Differential cross-section for inclusive prompt photon production measured with the ATLAS detector [7], compared with the predictions from the SHERPA generator assuming several energy thresholds for photon decay

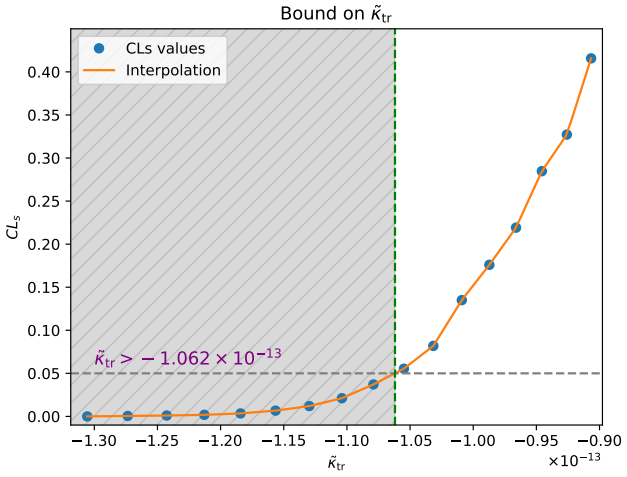

Figure 3: Bound on $\tilde{\kappa}_{tr}$ as a function of CL_s values.

tions, collider-based constraints offer a controlled experimental environment, reducing systematic uncertainties related to particle origins and propagation effects.

Looking forward, future high-energy colliders such as the FCC-hh [14], which is expected to operate at a center-of-mass energy of 100 TeV, could extend the sensitivity to Lorentz violation even further. Assuming the production of prompt photons up to approximately 20 TeV, the lower bound on $\tilde{\kappa}_{tr}$ could improve by two orders of magnitude, pushing the constraints on Lorentz violation to unprecedented levels. Additionally, further investigations into other sectors, such as top-quark production and decay processes, could provide complementary tests of Lorentz symmetry.

References

[1] D. Colladay and V. Kostelecký, *Cpt violation and the standard model*, *Phys. Rev. D* **55** (1997) 6760 [hep-ph/9703464].

[2] D. Colladay and V. Kostelecký, *Lorentz-violating extension of the standard model*, *Phys. Rev. D* **58** (1998) 116002 [hep-ph/9809521].

[3] V. Kostelecký and N. Russell, *Data tables for lorentz and cpt violation*, *Rev. Mod. Phys.* **83** (2011) 11 [0801.0287v16].

[4] D. Amram, K. Bouzoud, N. Chanon, H. Hansen, M. Ribeiro and M. Schreck, *New constraint for isotropic lorentz violation from lhc data*, *Phys. Rev. Lett.* **132** (2024) 211801.

[5] B. Altschul, *Vacuum cerenkov radiation in lorentz-violating theories without cpt violation*, *Phys. Rev. Lett.* **98** (2007) 041603 [hep-th/0609030].

[6] F. Klinkhamer and M. Schreck, *New two-sided bound on the isotropic lorentz-violating parameter of modified-maxwell theory*, *Phys. Rev. D* **78** (2008) 085026 [0809.3217].

[7] A. Collaboration, *Measurement of the inclusive isolated-photon cross section in pp collisions at $\sqrt{s} = 13$ tev using 36 fb^{-1} of atlas data*, *JHEP* **10** (2019) 203 [1908.02746].

[8] E.B. et al. [Sherpa], *Event generation with sherpa 2.2*, *SciPost Phys.* **7** (2019) 034 [1905.09127].

[9] F. Siegert, *A practical guide to event generation for prompt photon production with sherpa*, *J. Phys. G* **44** (2017) 044007 [1611.07226].

[10] A. Collaboration, *Measurement of the inclusive isolated prompt photon cross section in pp collisions at $\sqrt{s} = 8$ tev with the atlas detector*, *JHEP* **08** (2016) 005 [1605.03495].

[11] A. Read, *Presentation of search results: The cl_s technique*, *J. Phys. G* **28** (2002) 2693.

[12] D. Collaboration, *Measurement of the differential cross section for the production of an isolated photon with associated jet in $p\bar{p}$ collisions at $\sqrt{s} = 1.96$ tev*, *Phys. Lett. B* **666** (2008) 435 [0804.1107].

[13] M. Hohensee, R. Lehnert, D. Phillips and R. Walsworth, *Limits on isotropic lorentz violation in qed from collider physics*, *Phys. Rev. D* **80** (2009) 036010 [0809.3442].

[14] F. Collaboration, *Fcc-hh: The hadron collider: Future circular collider conceptual design report volume 3*, *Eur. Phys. J. ST* **228** (2019) 755.